Extended Abstracts of the 2012 International Conference on Solid State Devices and Materials, Kyoto, 2012, pp1023-1024

MIM Capacitors with High Capacitance Density and Low Quadratic Voltage Coefficient Employing Canceling Effect by $ZrLaO_x/ZrTiO_x/ZrLaO_x$ Laminate Insulator

Lun-Lun Chen, Yu-Bo Lin, Chia-Chun Lin, You-Tai Chang, and Yung-Hsien Wu*

Department of Engineering and System Science, National Tsing-Hua University, 300, Hsinchu, Taiwan
Phone:+886-3-516-2248 Email: yunhwu@mx.nthu.edu.tw

I. Introduction

For the past few years, metal-insulator-metal (MIM) capacitors have attracted intensive attention because of the wide applications for radio frequency (rf) and analog/mixed signal circuits. According to ITRS, the quadratic voltage coefficient of capacitance (VCC-α) <100 ppm/V^2 and capacitance density >12 fF/μm^2 are required for the RF passive technology by 2020. Although many high-permittivity (high-κ) dielectrics have been explored for MIM capacitors with capacitance density higher than 20 fF/μm^2, VCC-α less than 100 ppm/V^2 has been rarely achieved. Increasing the dielectric thickness is an effective way to improve the VCC-α, however, it comes at the price of degrading capacitance density. Recently, stacking two dielectrics respectively with a positive and a negative VCC-α has been proposed as a promising avenue to obtain a desirable VCC-α without sacrificing the capacitance density due to the so-called "canceling effect" [1]. To adopt this effect, it is prerequisite to find out a proper dielectric with negative VCC-α. However, most dielectrics demonstrate the characteristics of a positive VCC-α. Currently, SiO_2 is a well-known dielectric with a negative VCC-α and has been widely integrated with HfO_2 [1], Sm_2O_3 [2] or TiO_2 [3], attempting to implement high-performance MIM capacitors. Unfortunately, because of the relatively low κ value of SiO_2, achieving capacitance density larger than 12 fF/μm^2 while preserving an acceptable VCC-α is very challenging. Nevertheless Y_2O_3 with a higher κ value than SiO_2 has recently been reported to possess a negative VCC-α, the performance of Y_2O_3/HfTiO-based MIM capacitors [4] still has room to improve. In this work, $ZrTiO_x$ with even higher κ value was found to have a negative VCC-α and its application for MIM capacitors was investigated. By integrating $ZrTiO_x$ with $ZrLaO_x$ [5] which corresponds a positive VCC-α, MIM capacitors enjoying a high capacitance density of 14.6 fF/μm^2 and a low VCC-α of 33 ppm/V^2 has been realized and holds promising prospects to be used for next-generation high-performance MIM capacitors.

II. Experiment

Prior to the fabrication of MIM capacitors, a 500-nm SiO_2 was thermally grown on Si wafer as the isolation layer. Then, the TaN layer of 200 nm was deposited as the bottom electrode. The dielectric of $ZrLaO_x$ (5 nm)/$ZrTiO_x$ (5 nm)/$ZrLaO_x$ (5 nm) laminate was sequentially deposited by electron beam evaporation. To understand the electrical behavior and extract κ value of respective dielectric, single $ZrTiO_x$ or $ZrLaO_x$ of 10 or 15 nm was deposited on some samples. Afterward, all samples were annealed at 400 ^oC in the O_2 ambient for 20 min to strengthen film quality by reducing dangling bonds. Note that for samples with laminate structure, the O_2 annealing was performed on $ZrLaO_x/ZrTiO_x$ bilayer before the deposition of the top $ZrLaO_x$. Finally, the TaN metal of 200 nm was deposited by DC sputter as the top electrode. Besides electrical characterization for MIM capacitors with different split conditions, x-ray diffraction (XRD) was adopted to examine whether the dielectric crystalizes during annealing. Brief process flow and device structure are shown in **Fig. 1**.

III. Results and Discussion

Fig. 2 shows the zero-biased capacitances (C_0) for MIM capacitors with various split conditions measured at different frequencies. The κ value of the single $ZrLaO_x$ (10 nm) and $ZrTiO_x$ (15 nm) are extracted to be 25.8 and 22.5 respectively while C_0 of 14.6 fF/μm^2 can be achieved for MIM capacitors with $ZrLaO_x/ZrTiO_x/ZrLaO_x$ laminate. Note that apparent frequency dispersion in capacitance can be observed for MIM capacitors with single $ZrTiO_x$ while others correspond to relatively frequency-independent capacitance. The reason why MIM capacitors with single $ZrTiO_x$ suffer from more pronounced frequency dispersion can be attributed to the easily formed TaTiO interfacial layer [6] between TaN/$ZrTiO_x$ during annealing. The interfacial layer is a defective thin film with inferior quality which lowers the relaxation time and consequently results in a capacitance much dependent on frequency [7]. This phenomenon also explains that since $ZrTiO_x$ is sandwiched by $ZrLaO_x$, it does not directly contact electrode and therefore the undesirable TaTiO interfacial layer can be avoided. **Fig. 3** displays the XRD spectra of the single $ZrLaO_x$ and $ZrTiO_x$ films with 400 ^oC O_2 annealing. Since no diffraction peaks are found for these two films, it can be inferred that the $ZrLaO_x/ZrTiO_x/ZrLaO_x$ laminate remains amorphous after thermal treatment. **Fig. 4** shows the normalized capacitance-voltage (C-V) curves for MIM capacitors with single $ZrTiO_x$. The VCC-α is extracted to be -4861 ppm/V^2 for 15 nm $ZrTiO_x$ and -10614 ppm/V^2 for 10 nm $ZrTiO_x$. The results confirm that $ZrTiO_x$ indeed possess negative VCC-α which is inversely proportional to the square of the thickness. Displayed in **Fig. 5** are normalized C-V curves for MIM capacitors with single $ZrLaO_x$ (10 nm), single $ZrTiO_x$ (15 nm) dielectric, and $ZrLaO_x/ZrTiO_x/ZrLaO_x$ laminate. Since $ZrLaO_x$ shows a strong positive VCC-α, according to the "canceling effect", MIM capacitors with $ZrLaO_x/ZrTiO_x/ZrLaO_x$ laminate achieve a low VCC-α of 33 ppm/V^2 which is close to the effective VCC-α of 101 ppm/V^2 calculated from the theoretical equation of a stacked dielectric [1]. Combining the capacitance density of 14.6 fF/μm^2 and the low VCC-α of 33 ppm/V^2, the electrical characteristics of MIM capacitors with $ZrLaO_x/ZrTiO_x/ZrLaO_x$ laminate well meet the device requirement in 2020 set by ITRS. Illustrated in **Fig. 6** is the comparison of the leakage current for MIM capacitors with single $ZrTiO_x$ and $ZrLaO_x/ZrTiO_x/ZrLaO_x$ laminate under the same physical thickness. The leakage current measured at the voltage of -1 V is about 2.5×10^{-7} A/cm^2 for MIM capacitor with $ZrLaO_x/ZrTiO_x/ZrLaO_x$ laminate and the leakage current is comparable to those reported in the literatures [2-3]. Compared to MIM capacitors with single ZrTiO, the significantly suppressed leakage current for those with $ZrLaO_x/ZrTiO_x/ZrLaO_x$ laminate can be ascribed to two aspects. (1) The bandgap of $ZrLaO_x$ (4.2~5.8 eV) is larger than $ZrTiO_x$ (3.5~5.8 eV) [8]. (2) The inferior TaTiO interfacial layer [6] is avoided. The important device parameters for MIM capacitors with various electrodes and dielectrics are summarized in **Table I**. Compared to the other high-κ capacitors [2-4, 9-10], MIM capacitors with

$ZrLaO_x/ZrTiO_x/ZrLaO_x$ laminate developed in this work reveal the best device performance and show the exceptional competence. Further improvement in leakage current is under investigation by employing NH_3 or O_2 plasma treatment for the laminate and the results will be reported elsewhere.

IV. Conclusion

The $ZrTiO_x$ film with a κ value of 22.5 was found to have a negative VCC-α. To fully exert the "canceling effect" of VCC-α, stacking $ZrTiO_x$ with $ZrLaO_x$ which corresponds to a positive VCC-α, dielectric in the structure of $ZrLaO_x/ZrTiO_x/ZrLaO_x$ was investigated in this work. Besides a high capacitance density of 14.6 fF/μm^2, a low VCC-α of 33 ppm/V^2 and an acceptable leakage current have been achieved. The results meet the ITRS requirement set for 2020 and the $ZrLaO_x/ZrTiO_x/ZrLaO_x$ laminate holds the great potential to be applied to next-generation high-performance MIM capacitors.

Acknowledgements

This work was supported by the National Science Council of Taiwan under Contract NSC 100-2221-E-007-102 and NSC 100-2120-M-009-007

References

[1] S. J. Kim et al., IEEE EDL, **25**, 538, 2004. [2] J. J. Yang et al., IEEE EDL, **30**, 460, 2009. [3] Y. H. Wu et al., IEEE EDL, **33**, 104, 2012. [4] B. Y. Tsui et al., IEEE EDL, **31**, 875, 2010. [5] Y. H. Wu et al., APL, **98**, 013506, 2011. [6] H. H. Hsu et al., Proc. Int. Symp. VLSI Technol., Syst., Appl., 67, 2009. [7] P. Gonon and C. Vallée., APL, **90**, 142906, 2007. [8] G. D. Wilk et al., JAP, **89**, 5243, 2001. [9] V. Mikhelashvili et al., APL, **92**, 132902, 2008. [10] T. H. Phung et al., J. Electrochem. Soc., **158**, H1289, 2011.

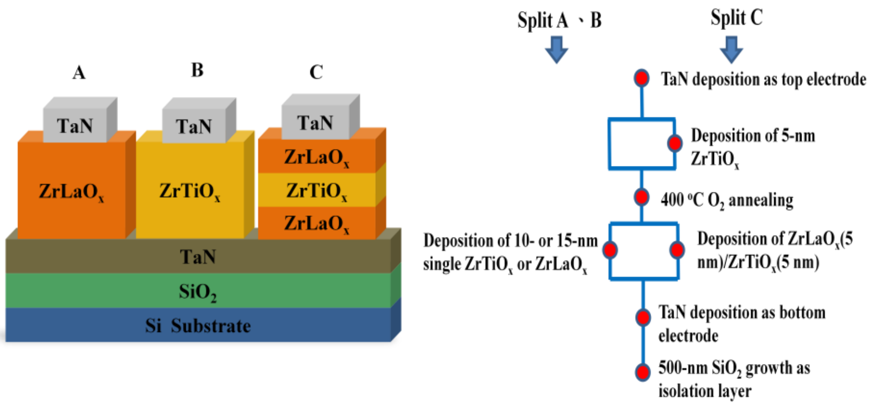

Fig. 1 Structure (not to scale) and process flow of MIM capacitors.

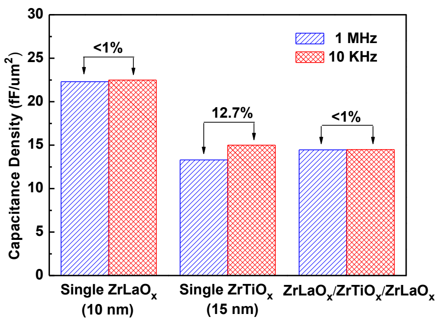

Fig. 2 C_0 for all samples with different process condition measures at 1 MHz and 10 KHz. The difference of C_0 between 1 MHz and 10 KHz is also displayed.

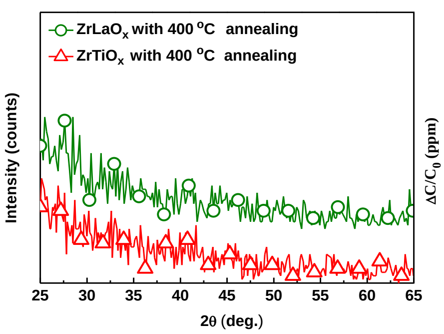

Fig. 3 XRD spectra for single $ZrTiO_x$ and $ZrLaO_x$ film with 400 °C annealing.

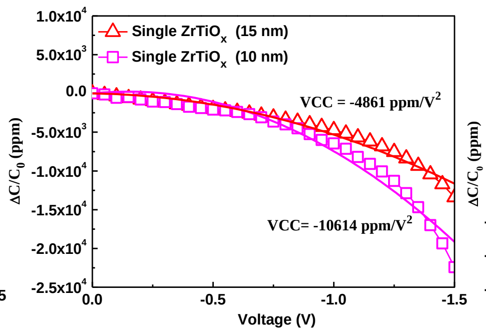

Fig. 4 Normalized C-V curves for single $ZrTiO_x$ with various thicknesses where C_0 is the zero-biased capacitance.

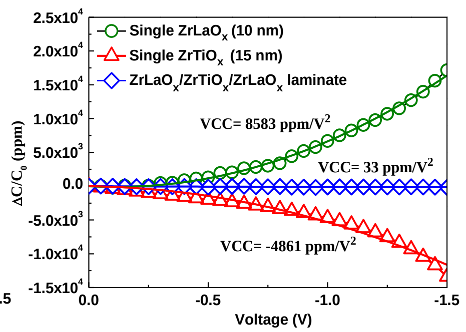

Fig. 5 Δ C/C_0 vs voltage for MIM capacitors with different process conditions where C_0 is the zero-biased capacitance.

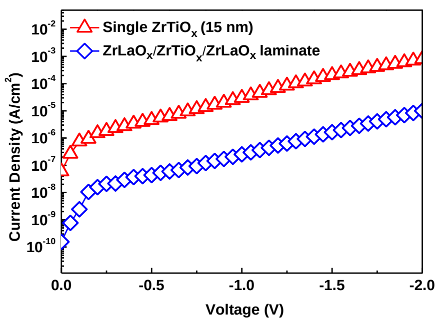

Fig. 6 Comparison of I-V characteristics for samples with different process conditions.

Material	Sm_2O_3/SiO_2 [2]	TiO_2/SiO_2 [3]	$HfTiO/Y_2O_3$ [4]	$HfN_xO_y/SiO_2/HfTiO_y$ [9]	Er_2O_3/SiO_2 [10]	This Work
Top Electrode	TaN	Al	Pt	Ta	TaN	TaN
Bottom Electrode	TaN	TaN	TaN	Pt	TaN	TaN
Work-function (eV)	4.6	4.6	5.6	4.2	4.6	4.6
Capacitance density (fF/μm^2)	7.9	11.9	11.2	11	7	14.6
VCC (ppm/V^2)	−56	90	1222	235	−73	33
J(A/cm^2)	2×10^{-7}@3.3 V	9.3×10^{-8}@1.8 V	6.4×10^{-9}@-1 V	1.5×10^{-7}@1.5 V	1×10^{-8}@3.3 V	2.5×10^{-7}@-1 V

Table I. Comparison of MIM capacitors with various stacked dielectric and top/bottom electrodes.